TELKOMNIKA Telecommunication, Computing, Electronics and Control
Vol. 19, No. 1, February 2021, pp. 134~145
ISSN: 1693-6930, accredited First Grade by Kemenristekdikti, Decree No: 21/E/KPT/2018
DOI: 10.12928/TELKOMNIKA.v19i1.16566

Improved myoelectric pattern recognition of finger movement using rejection-based extreme learning machine

Khairul Anam[1], Adel Al-Jumaily[2]
[1]Department of Electrical Engineering, Faculty of Engineering, University of Jember, Indonesia
[2]School of Electrical, Mechanical and Mechatronic Systems, Faculty of Engineering and Information Technology, University of Technology Sydney, Australia

Article Info

Article history:

Received May 1, 2020
Revised Aug 10, 2020
Accepted Sep 15, 2020

Keywords:

Extreme learning machine
Finger movement
Hand exoskeleton
Myoelectric pattern recgnition

ABSTRACT

Myoelectric control system (MCS) had been applied to hand exoskeleton to improve the human-machine interaction. The current MCS enables the exoskeleton to move all fingers concurrently for opening and closing hand and does not consider robustness issue caused by the condition not considered in the training stage. This study addressed a new MCS employing novel myoelectric pattern recognition (M-PR) to handle more movements. Furthermore, a rejection-based radial-basis function extreme learning machine (RBF-ELM) was proposed to tackle the movements that are not included in the training stage. The results of the offline experiments showed the RBF-ELM with rejection mechanism (RBF-ELM-R) outperformed RBF-ELM without rejection mechanism and other well-known classifiers. In the online experiments, using 10-trained classes, the M-PR achieved an accuracy of 89.73% and 89.22% using RBF-ELM-R and RBF-ELM, respectively. In the experiment with 5-trained classes and 5-untrained classes, the M-PR accuracy was 80.22% and 59.64% using RBF-ELM-R and RBF-ELM, respectively

Corresponding Author:

Khairul Anam
Department of Electrical Engineering
University of Jember
Kalimantan 37 St, Jember, East Java, Indonesia
Email: khairul@unej.ac.id

1. INTRODUCTION

Many countries have a significant number of people with disability. The results of the Survey of Disability, Ageing and Carers (SDAC) in 2009 showed that four million people in Australia (18.5%) suffer from disability. Stroke is one of the major factors causing disability in Australia. In 2009, it was estimated that 1.8% of Australians have suffered from a stroke. Of the people who are impaired due to stroke, 62% reported that stroke is the primary cause of disability. About 40% of them have difficulties using their arms or fingers or difficulties in gripping [1].

Inevitably, hand disability caused by stroke has decreased the quality of life for individuals and carers. Therefore, many attempts have been made to tackle this problem through traditional therapy or even advanced technology such as robot technology [2-5]. The hand exoskeleton, as a part of robotic devices, becomes the best solution to recovering the quality of life for the following reasons. It is portable and worn by the subject so that the therapy can be done anywhere and anytime. Besides, it is easy to be equipped with an interactive interface such as a game technology to enhance the effectiveness of the therapy.

The hand exoskeleton is expected to help the wearer comfortably. Therefore, a user does not feel uncomfortable and have trouble when doing a motion task while wearing it. In other words, the assistance should be provided as needed [6, 7]. To attain such a smooth interaction, the control system of the robot should consider the human intention. However, developing such a control method is not an easy task. Different biological signals have been considered to detect the user's intention. Myoelectric signal (MES) or electromyography (EMG) signal that contains sufficient information of the user's intention has been used to control rehabilitation devices or assistive robots for years. Myoelectric control has been implemented in two ways: non-pattern recognition and pattern recognition [8]. In the first application, the EMG signal has been utilized to detect force or any physical information such as angle to control the exoskeleton devices [9-11]. The second type of EMG implementation is the EMG-based pattern recognition. It has been done by analyzing the EMG signals and classifying the correct movement from predefined sets of limb movements. Different types of movements have been studied so far such as hand [12-19] and leg [20, 21] movements.

Some hand exoskeletons have employed surface EMG to come up with a smooth human-machine interaction. Mulas *et al.* [22] have developed a hand exoskeleton controlled by EMG signal. The EMG signal collected from the subject's forearm is used to predict the user's intention to move or not to move. This information was employed to drive fingers of the hand exoskeleton or keep them in a rest state. All fingers excluding the thumb are controlled simultaneously. Furthermore, Wege and Zimmermann [23] have developed myoelectric control system (MCS) for a hand exoskeleton that could move an individual finger based on the user's intention. The MCS utilizes EMG electrodes to acquire electrical activities from 16 muscles. Moreover, the control system employs a blind source separation to separate the information contained in the high-density surface EMG signals at the forearm into several signals related to a specific finger movement. However, the experimental result is not satisfying.

The latest MCS for the hand exoskeleton is the one developed by Ho *et al.* [24]. The exoskeleton's structure fits different finger lengths and aligns with the virtual center of rotation of the metatarsophalangeal (MCP) and the proximal interphalangeal (PIP). This device is able to detect the user's intention from the user's muscle for hand opening and closing. Thus, this device is able to drive all the finger movements simultaneously to open and close the hand. The aforementioned facts show that the workable myoelectric controller on the current hand exoskeleton deals with simple finger movements, i.e. simultaneous finger movements such as opening and closing the hand. Moreover, the present EMG-based controller is designed to recognize the movements that are involved in the training. However, it fails to recognize the movements that are not included in the training stage [25]. In real-time application, the trained movements are limited, yet the untrained movements are many. As a result, the performance of the MCS decreases when it works in real-time or clinical application.

In summary, two main problems appear in the current MCS for the hand exoskeleton. The first is related to the limited number of finger movements that can be dealt with. The second is related to the capability of the MCS to reject the untrained movements that possibly appear in the real-time application. This paper proposes a new MCS for the hand exoskeleton that overcomes these two issues. The improved MCS that is proposed employs the EMG-based pattern recognition (EMG-PR) to enable complex finger movements, instead of hand opening and closing. Furthermore, to cope with the untrained movement issue, this paper proposes a classifier called radial basis function extreme learning machine [26] with rejection mechanism (RBF-ELM-R). RBF-ELM-R detects the untrained movements and rejects them. In other words, the system will consider the rejected movements as a no-action or a rest state. The paper is organized as follows; section 2 provides a description of the basic concept of RBF-ELM with rejection mechanism (RBF-ELM-R). Section 3 presents the proposed MCS. Section 4 provides the experimental result and statistical analysis for the offline and online classification of the proposed system on the hand exoskeleton. Section 5 presents the conclusion.

2. REJECTION-BASED EXTREME LEARNING MACHINE

2.1. Extreme learning machine

Extreme learning machine (ELM) is an exceptional innovation of single-layer feed-forward neural network (SLFN), which overcomes shortcomings of the neural network, especially in the processing time. It omits an iterative learning process by setting the hidden node weight randomly and calculating the output weight analytically. Therefore, the training time is extremely fast when compared with the traditional neural networks. Interestingly, the hidden node part can be constructed using either original nodes or a kernel function [26].

The output function of ELM for a generalized SLFN (for one output node case) is:

$$f(x) = \sum_{i=1}^{L} \beta_i h_i(x) = h(x)\beta \qquad (1)$$

where $\beta = [\beta_1, \ldots, \beta_L]^T$ is the vector of the output weight between the hidden layer of L nodes and the output node, h(x) = $[h_1(x), \ldots, h_L(x)]$ is the output vector of the hidden layer. The objective of ELM is to minimize the error and the norm of weight:

$$Minimize: \|H\beta - T\|^2 and \|\beta\| \tag{2}$$

where T is the target. For the classification purpose, the output of ELM as shown in (1) could be modified as:

$$f(x) = h(x)\beta = h(x)H^T \left(\frac{1}{C} + HH^T\right)^{-1} T \tag{3}$$

where

$$H = \begin{bmatrix} h(x_1) \\ \vdots \\ h(x_N) \end{bmatrix} = \begin{bmatrix} h_1(x_1) & \cdots & h_L(x_1) \\ \vdots & \vdots & \vdots \\ h_1(x_N) & \cdots & h_L(x_N) \end{bmatrix} \tag{4}$$

and C is a user-specified parameter, L is the number of the hidden unit, and N is the number of the training data. The parameters C and L should be chosen properly to achieve good generalization performance. However, there is no specific method to determine both parameters except trial and error. Fortunately, Huang *et al.* [26] proved that the big number of L gives a good performance so that the users just need to determine the parameter of C. Furthermore, in (4), h(x) is a feature mapping (hidden layer output vector).

2.2. Radial basis ELM

If the feature mapping h(x) is unknown to the user, a kernel function can be used to represent h(x). Then, as shown in (3) would be:

$$\begin{aligned} f(x) &= \mathbf{h(x)H}^T \left(\frac{1}{C} + \mathbf{HH}^T\right)^{-1} \mathbf{T} \\ &= \begin{bmatrix} K(x, x_1) \\ \vdots \\ K(x, x_N) \end{bmatrix} \left(\frac{1}{C} + \Omega_{ELM}\right)^{-1} \mathbf{T} \end{aligned} \tag{5}$$

where

$$\Omega_{ELM} = HH^T : \Omega_{ELM_{i,j}} = h(x_i).(x_j) = K(x_i, x_j) \tag{6}$$

and K is a kernel function. Following our work results [27, 28], this paper employed a radial basis function (RBF) kernel and it is called radial basis function extreme learning machine (RBF-ELM). The RBF kernel is defined as

$$K(u, v) = exp(-\gamma\|u - v\|^2) \tag{7}$$

2.3. RBF-ELM-R

To reject the movements that are not trained or involved in the training section or even the movements that may be out of physical limitation, a rejection mechanism is added to the RBF-ELM. The rejection mechanism is conducted based on the confidence level of the output of RBF-ELM. The output is accepted if the confidence level is higher than the predefined threshold value. This value is derived from the experimental procedures that differentiate the rest state and the finger movements. Otherwise, the output will be rejected if the confidence level is lower than the predefined threshold value. The confidence level is calculated using entropy [29] and defined by;

$$E(n) = \sum_j^{N\Sigma(o_j(n))} o_j(n) ln \tag{8}$$

where N is the number of the output unit, n is the iteration of data, and Oj is the jth output of the output layer of ELM. The low entropy indicates that the probability of a specific output can clearly be differentiated from others. On the other hand, high entropy implies that the probabilities of the outputs are similar or very close to each other so that there is ambiguity in determining the correct output.

3. THE PROPOSED MYOELECTRIC CONTROL FOR THE HAND EXOSKELETON

This paper proposes a novel MCS for the hand exoskeleton with minimum channel reading. The MCS consists of two main parts, the myoelectric pattern recognition (MPR) and non-pattern recognition blocks (M-non-PR), as depicted in Figure 1. Using just two EMG channels, the MPR produces the intended finger motion that the robot should perform and the M-non-PR estimates the strength of the intended movement. However, in this paper, all experiments involved only one level of strength, which is maximum voluntary contraction (MVC).

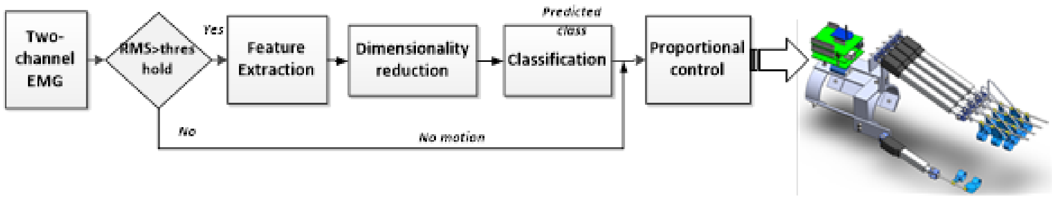

Figure 1. Myoelectric control system developed to control the hand exoskeleton

3.1. Data aquisition

The FlexComp Infiniti™ System from Thought Technology was used to acquire the signals from two EMG sensors, MyoScan™ T9503M, that were put on the subject's forearm as seen in Figure 2. The acquired EMG signals were amplified with a total gain of 1000 and sampled at 2000 Hz. A band-pass filter between 20 Hz and 500 Hz filters the collected EMG signals. Besides, a notch filter was employed to remove the 50 Hz line interference. Before being applied to the hand exoskeleton, the MCS was tested in the offline experiment to examine and verify the efficacy of the proposed system. Eight subjects were involved consisting of 2 females and 6 males aged 24-60 years. All subjects were normally limbed with no muscle disorder. The subjects were asked to perform a particular posture of finger movement for 5s and then take rest for 5s. Each action was repeated six times.

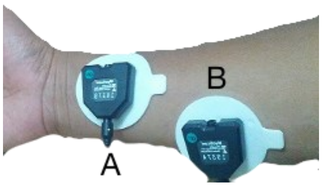

Figure 2. Placement of the electrode A (flexor policis longus) and electrode B (flexor digitarium superficialis)

3.2. Myoelectric patern recognition

Figure 3 describes the myoelectric pattern recognition (MPR) using rejection-based ELM. The proposed system evaluates the amplitude of the EMG signals to detect the motion intention of the user. To do so, the average of root mean square (RMS) from two channels is compared with the threshold value. If the mean is lower than the threshold value, this produces "no motion". Otherwise, the MPR will be activated and generates the intended movement. In more detail explanation from feature extraction to post-processing, the following will illustrate it.

As stated in Tkach *et al.* [30] that the coefficients of autoregressive (AR) model and time-domain (TD) features were stable and robust to the electrode location shift and the change of signal level, this paper extracted features from the TD feature and coefficients of the autoregressive model. The TD features consisted of mean absolute value (MAV), slope sign changes (SSC), waveform length (WL), and zero crossings (ZC). In addition, the parameters of Hjorth time domain parameters were added to improve the performance of the system [31]. The features were extracted with duration of 100 ms every 100 ms. After features were extracted from all EMG channels, they were then concatenated to form a large feature set. As a result, the dimension of the feature set is large. Therefore, the dimension was reduced and at the same time projected to new features that are more separable. This paper utilized spectral regression discriminant analysis (SRDA), following the recommendation of previous work [28]. SRDA is an extension of linear discriminant analysis (LDA) that can improve the performance of LDA in terms of speed and ability to work on a large dataset [32].

To enhance the classification performance, the proposed MCS introduces a rejection mechanism into radial basis function extreme learning machine or as it is called RBF-ELM-R. To investigate and verify the performance of RBF-ELM-R, offline classification was conducted. In the offline classification, the performance of RBF-ELM-R was compared with the original RBF-ELM and other well-known classifiers such as support vector machine (SVM), least-square support vector machine (LS-SVM), linear discriminant analysis (LDA), and k-nearest neighbor (kNN). There were 10 classes involved in the experiments. These 10 classes consist of 5 individual finger movements, 4 combined finger movements, and hand-close (HC) movement. The individual finger movements involve thumb (T), index (I), middle (M), ring (R), and little (L) fingers. The four combined movements were the pinching of thumb and index (T-I), thumb and middle (T-M), thumb and ring (T-R), and thumb and little (T-L). The classifier sometimes misclassifies the movement into wrong movements. The post-processing that is conducted after the classification can overcome this issue. A majority vote [33] is one of the post-processing methods that can be used to smoothen the classification results. It employs the output from the present state and previous states and produces a new classification result based on the class that appears most frequently. This procedure produces the finger movement class that removes fake misclassifications.

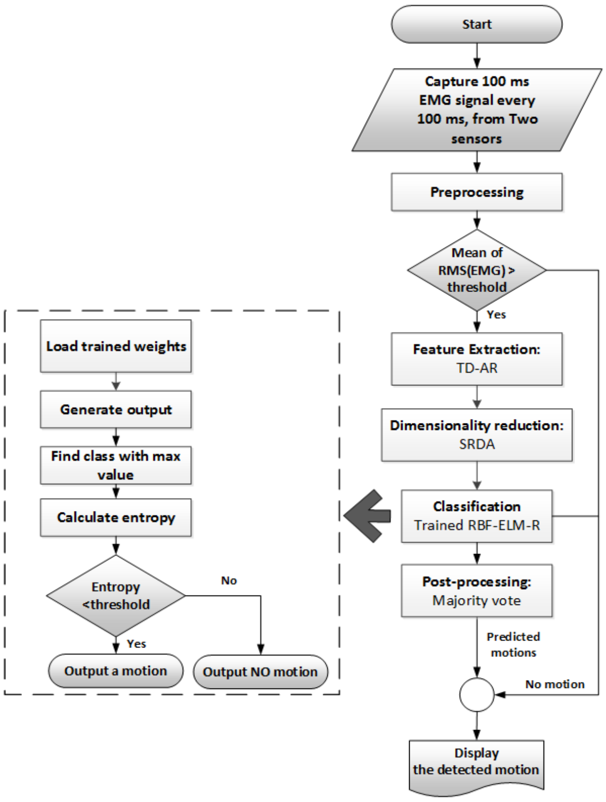

Figure 3. The proposed myoelectric pattern recognition

3.3. Myoelectric non-patern recognition

The main component of MCS is the myoelectric pattern recognition (M-PR). Nevertheless, the MCS also consists of the myoelectric non-pattern recognition (M-non-PR) to detect the strength of the intended movement. However, the M-non-PR is not discussed in this paper. All experiments consider the MVC. The M-non-PR system has similar steps as the M-PR except in the classification stage. As seen in Figure 1, the M-non-PR estimates the strength of the signal by getting the root mean square (RMS) values of all the EMG channels. Then, the average of RMS values is calculated and sent to the proportional controller.

3.4. Proportional controller

In this proportional controller, the control signal for the hand exoskeleton is proportional to the contraction level of the EMG signal. If the intended motion is detected, then the motor command is sent to the robot. The amplitude of the robot motion is proportional to the contraction level of the EMG signal. If the contraction level exceeds the MVC, then the MVC will be used as the motor command.

3.5. The hand exoskeleton

The proposed MCS was applied to the hand exoskeleton developed in our previous work [34]. The hand exoskeleton is able to flex fingers actively at the metacarpophalangeal (MCP) joint and passively at the proximal interphalangeal (PIP) and distal interphalangeal (DIP) joint. The Arduino microcontroller board was used to drive the five linear DC motors for actuating the hand exoskeleton as described in Figure 1 and Figure 4. The hand exoskeleton did not have any sensors, neither force nor angle sensors. The hand exoskeleton merely relied on the EMG sensors.

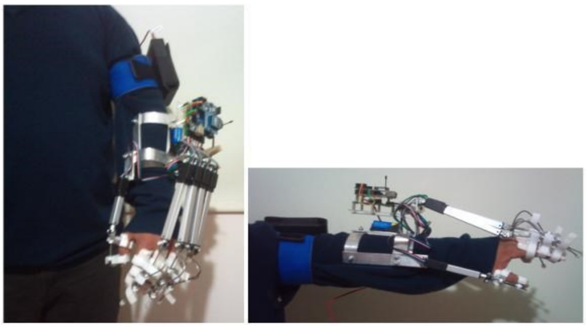

Figure 4. The hand exoskeleton used in the experiment

4. RESULT AND ANALYSIS

This section presents the results of offline and online experiments. Offline experiment was conducted to investigate the performance of the proposed MCS, in particular the myoelectric pattern recognition using RBF-ELM-R. Meanwhile, online experiment was aimed at applying the proposed MCS to the hand exoskeleton. To test the proposed method, comparison with other well-known classifiers was also carried out.

4.1. Offline experiment

4.1.1. The perfrmance of RBF-ELM-R

In the offline experiment, the paper investigates the effectiveness of the rejection mechanism in RBF-ELM-R and its implication on the performance of the myoelectric pattern recognition system. As seen in Tables 1 and 2, all experiments used six categories from 10 classes. Each of them consists of trained and untrained classes ranging from 5 and 5 to 10 and 0, respectively. When the M-PR was trained using 5 trained classes for testing data, the remaining 5 classes were used for training data. This will continue from the first category to the sixth. In addition, threshold value varied from 0.1 to 1.0 with increment 0.1.

Furthermore, this paper investigates the performance of the system that utilizes the rejection mechanism and compares it with the system without the rejection mechanism. Since this study conducted 10 classes in which each has trained and untrained classes, three-fold cross validation was used. This means that when about 30% of the data is used for testing, the remaining is for training. Figure 5 and Table 1 present the experimental results.

Figure 5 and Table 1 indicate that M-PR with small threshold values achieved high accuracy. In addition, the system that is trained using 5 classes and then tested using 5 untrained classes achieved poor accuracy. Another interesting fact provided in Table 1 is that the system without rejection mechanism (RBF-ELM) and with rejection mechanism (RBF-ELM-R) experienced poor performance when the untrained classes were imposed into the system. The accuracy of RBF-ELM on 10 trained classes was 87%. However, the accuracy dropped to 65.9% when one untrained class was introduced to the system (as can be noticed in the dark-gray background in Table 1. Fortunately, the system with rejection mechanism (RBF-ELM-R) could improve the dropped accuracy of RBF-ELM due to the existence of the untrained classes in the testing stage by around 10%, when using threshold 1.0. Similar improvement also occurred in all cases, but the enhancement became less by increasing the number of untrained classes in the testing.

In addition to Table 1, Table 2 describes the accuracy when the rejection mechanism is combined with the majority vote. It seems that the majority vote decreases the accuracy of the system with the rejection mechanism, especially for low threshold values. The rejection rate of the low threshold value is high so that the majority vote does not have enough data to vote the correct outputs. Therefore, the majority vote is not appropriate to be implemented on the rejection-based classifier, especially for the low threshold values.

Table 1. The accuracy achieved across eight subjects using six-fold cross-validation without using the majority vote

#classes		Rejection with threshold (accuracy %)										
Train- ed	Un- trained	0.1	0.2	0.3	0.4	0.5	0.6	0.7	0.8	0.9	1.0	No Rejection
5	5	71.0	60.1	49.3	43.8	38.1	34.1	31.2	28.4	26.5	**25.4**	**23.8**
6	4	74.5	74.6	61.2	56.2	51.6	47.4	43.7	40.1	36.6	**34.6**	**30.8**
7	3	NA	87.7	75.4	68.5	63.7	58.6	55.0	51.2	47.6	**44.7**	**39.5**
8	2	NA	94.1	88.5	79.0	75.0	70.8	67.8	64.6	61.7	**58.7**	**51.1**
9	1	NA	97.8	95.4	89.1	85.9	84.8	83.4	81.2	78.5	**75.9**	**65.9**
10	0	NA	NA	99.6	99.0	98.6	98.4	98.1	97.4	96.2	**94.6**	**87.0**

Table 2. The accuracy achieved across eight subjects using six-fold cross-validation using the majority vote

#Classes		Rejection with threshold (accuracy %)										No Rejection
Trained	Un-trained	0.1	0.2	0.3	0.4	0.5	0.6	0.7	0.8	0.9	1.0	
5	5	43.1	55.7	46.8	42.0	36.7	33.1	30.4	28.0	26.3	**25.2**	**23.6**
6	4	46.6	64.2	56.7	53.2	49.2	45.5	42.4	39.3	36.2	**34.4**	**30.8**
7	3	NA	62.0	67.2	63.5	60.1	56.0	53.1	50.1	47.2	**44.7**	**40.1**
8	2	NA	50.2	74.0	71.4	69.6	66.9	64.9	62.5	60.6	**58.4**	**52.3**
9	1	NA	59.1	70.7	77.7	78.4	79.3	79.2	78.1	76.5	**75.2**	**68.1**
10	0	NA	NA	63.2	81.6	87.6	90.5	92.1	92.7	93.0	**92.9**	**90.5**

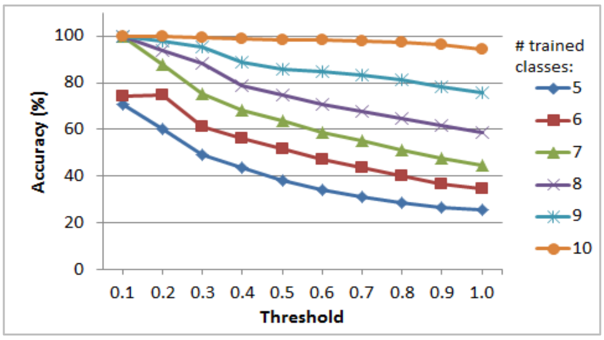

Figure 5. Variation of rejection threshold on the system performance without majority vote

Furthermore, Figure 5 indicates that the smaller the threshold value is, the more accurate the system is. However, the rejection rate of the system should be considered properly to determine the optimal threshold value and avoid wrong rejection. Table 3 can be used to find the optimal threshold value for each case. In the experiment that used 5 trained classes, the percentage of the untrained data is 75%. It implies that the system with rejection mechanism could reject the output by a rejection rate around or less than this value. Therefore, threshold ranging 0.2-0.4 can be the optimal solution for this case. Similarly, if the same procedure is applied, the gray background in Table 3 presents the possible threshold values for different cases.

Looking at Tables 1 and 2, the data presented prove that the motion rejection in the myoelectric control improves the performance of the system. Figure 6 shows a detailed comparison between the two systems, RBF-ELM and RBF-ELM-R, on the 10-classes experiment. The figure clearly indicates that RBF-ELM-R outperforms RBF-ELM on all subjects without exception. RBF-ELM attained accuracy of around 90% while RBF-ELM-R is around 92%. The superiority of RBF-ELM-R over RBF-ELM is more obvious when one-way ANOVA test is conducted. By setting p at 0.05, the p-value was 0.034, which was less than 0.05. Therefore, the enhancement made by RBF-ELM-R is statistically significant.

Table 3. The rejection rate of threshold experiments on eight subjects using threefold cross-validation

# Trained classes	Untrained classes (%)	Threshold (rejection rate %) 0.1	0.2	0.3	0.4	0.5	0.6	0.7	0.8	0.9	1.0
5	75	89.6	**80.1**	**64.7**	**56.0**	47.4	38.8	32.0	24.2	15.6	10.7
6	60	99.5	88.9	**71.9**	**62.1**	**52.6**	43.1	35.5	26.9	17.4	11.9
7	45	100	95.3	80.9	70.1	**60.2**	**49.0**	**40.5**	32.4	23.2	15.8
8	30	100	98.1	86.5	73.4	63.2	52.7	**43.5**	**36.0**	**27.9**	20.4
9	15	100	99.3	91.3	77.6	66.6	56.4	46.3	38.5	**30.7**	**23.4**
10	0.0	100	100	94.2	81.0	69.6	58.4	47.5	38.8	31.6	**23.9**

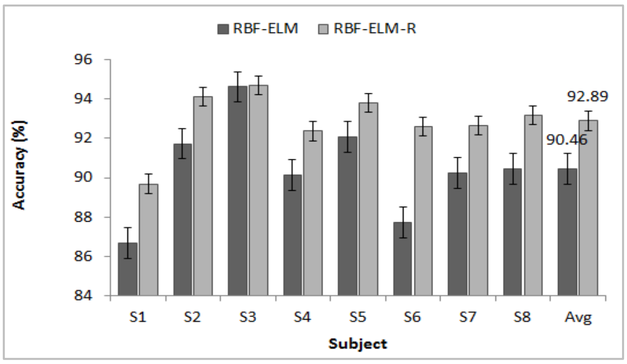

Figure 6. Accuracy achieved by RBF-ELM and RBF-ELM-R (threshold = 1.0) across eight subjects using threefold cross-validation using majority vote

4.1.2. RBF-ELM-R and other classifiers

This experiment examines the performance of RBF-ELM-R in comparison with certain well-known classifiers such as support vector machine (SVM), least-square SVM (LS-SVM), linear discriminant analysis (LDA), and k-nearest neighbor (kNN). The experimental results are described in Figure 7 and Table 4. Figure 7 shows that RBF-ELM-R with the rejection threshold 1.0 attained the best accuracy of all classifiers across different class numbers. The accuracy of all classifiers decreased as the number of trained classes decreased while the number of untrained classes increased. No classifiers could cope with this situation, in particular in the 5-trained class experiment.

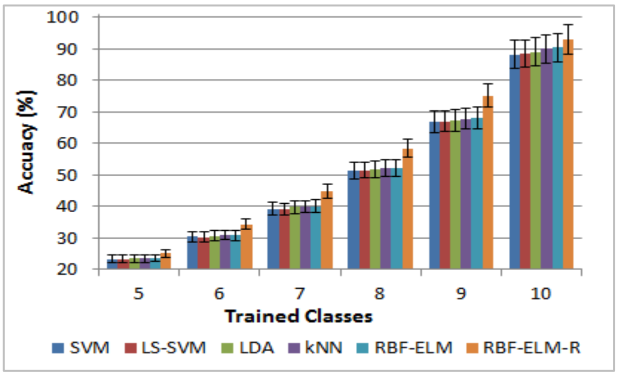

Figure 7. Accuracy of RBF-ELM-R (with rejection threshold 1.0) compared with other well-known classifiers

Table 4. Accuracy of the real-time experiment using 10 trained classes using majority vote

# Trained Classes	Accuracy (%) SVM	LS-SVM	LDA	kNN	RBF-ELM	RBF-ELM-R
5	23.36	23.43	23.53	23.59	23.64	25.20
6	30.42	30.31	30.77	30.90	30.84	34.40
7	39.26	39.06	39.82	39.95	40.07	44.70
8	51.35	51.54	51.71	52.16	52.26	58.40
9	66.85	67.06	67.20	67.84	68.07	75.20
10	88.26	88.52	88.99	90.03	90.46	92.90

This is the fact of the real-time application; the number of movements that are not involved in the training section is much larger than those that are participating in the training section. The advantage of RBF-ELM-R is highlighted in this situation. By varying the rejection threshold, the performance of the M-PR can be improved. Looking at Table 1 in the case of the 5-trained classes (first row), if the rejection threshold is decreased from 1.0 to 0.2, the accuracy of RBF-ELM can be enhanced from 25.4% to 60.1%.

4.2. Online experiment

The result of the offline experiments concludes that the system with rejection mechanism could enhance the classification performance, especially when the untrained movements are introduced in the testing stage. In this experiment, the result of the offline classification was applied to the real-time application to control the hand exoskeleton. In the online experiment, an able-bodied user wore the hand exoskeleton on the left hand. On the right hand, there were two EMG sensors placed on the forearm, as shown in Figure 8. This is done since many people may suffer from one side motor function deficiency of the body (hemiparesis).

Figure 8 exhibits the example of the real-time experiments on the hand exoskeleton on the able-bodied subject. The figure only provides 6 movements. In the experiment, 10 movements were tested as well. In this experiment, the subject performed 10 subsequent movements from the thumb, index finger until the hand-close movement. The duration of each movement is 5 s with a rest state in between lasting 2.5 s.

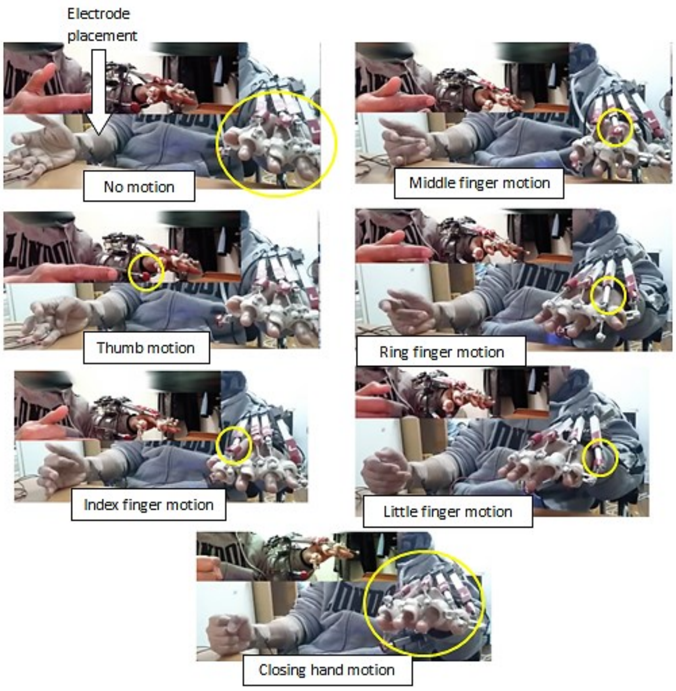

Figure 8. An example of the online experiment of myoelectric pattern recognition with motion rejection on the exoskeleton hand

There are two scenarios involved. The first scenario is when all 10 movements are included in the training and testing sessions. As for the second scenario, 5 individual movements are involved in the training session. However, in the testing session, the trained system is tested with 10 finger movements: 5 individual fingers and 5 combined fingers. In addition, the subject repeated the experiment four times. The performance of the system is presented in Table 5.

The experiment results in Table 5 show that the average accuracy of the real-time application across the four trials is 89.22% and 89.72% using RBF-ELM and RBF-ELM-R, respectively. In online experiment, the experiment on 5 trained classes and untrained classes was also conducted. The results are presented in Table 5 (on the right-hand side). Table 5 shows that the rejection mechanism could minimize the performance degradation of the real-time myoelectric pattern recognition (M-PR). The M-PR using RBF-ELM-R could achieve the accuracy of about 80% while the one using RBF-ELM attained the accuracy of about 59%.

Table 5. Accuracy of the real-time experiment

Trials	10 Trained classes		5 Trained classes and 5 untrained classes	
	RBF-ELM	RBF-ELM-R	RBF-ELM	RBF-ELM-R
1	89.06	90.46	59.38	82.01
2	89.45	89.75	60.55	79.07
3	90.23	90.06	60.29	81.45
4	88.15	88.64	58.33	78.35
Mean	89.22	89.73	59.64	80.22

The timing diagram of the online experiment on 5 trained classes and untrained classes is presented in Figure 9. The figure presents the outputs of myoelectric pattern recognition using three different scenarios. The first scenario is the output of RBF-ELM, i.e. the system that does not use the rejection mechanism. It is shown in the figure by the letter A. The second scenario is the output of RBF-ELM-R with rejection threshold 0.3, which is shown by the letter B in the figure. The last scenario, which is shown by the letter C, is the output of RBF-ELM-R with rejection threshold 0.3, but it employed different concepts of "no motion" from the previous RBF-ELM-R. The rejection motion in RBF-ELM-R could be applied in two ways depending on the implementation of "no motion." First, "no motion" means that the output of the system was a rest state. Therefore, whenever the system rejects a motion, the system forced the output to the rest state by neglecting the current movement. As a result, the output changed from one state to a rest state back and forth frequently, as shown in Figure 9, part B. Unfortunately, this action will be inconvenient for the users. The second implementation of "no motion" was that, instead of the rest state, the output was the last movement produced before the implementation of the rejection mechanism. This scenario produced smoother output than the first scenario, as shown in Figure 9, part C. For this reason, the second scenario was a good choice for controlling the hand exoskeleton. However, there is a drawback when using the previous state as "no motion." When the previous state is the wrong movement, then the "no motion" produces the wrong movement as well. For example, see Figure 9, part C, the thumb-index finger movement (TI) is a motion that was not included in the training stage. When it is imposed on the system, the system outputs the L movement. In fact, the correct output should be no movement.

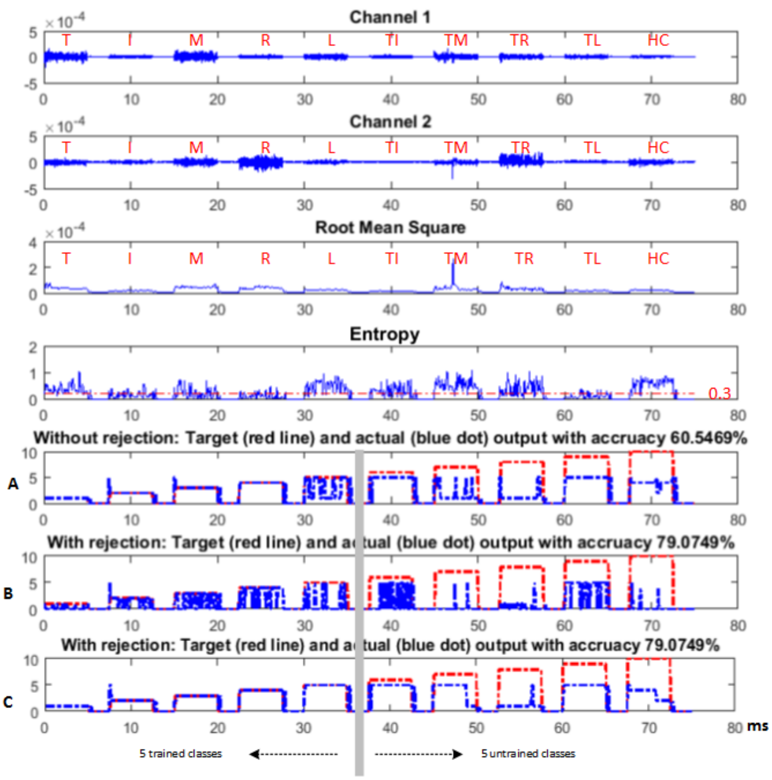

Figure 9. Real-time experiment results over time using threshold 0.3 using 5 trained classes and 5 untrained classes

4.3. Limitation of the work

The work in this paper has some limitations. First, the experiments conducted in this paper worked on the movement at MVC. Actually, the non-pattern recognition method has been developed to measure the contraction level of the EMG signal. However, it was not discussed in detail. In future experiments, different levels of contraction of the movements should be considered to test the reliability of the proposed system in the real application. The second limitation of this work is the fact that the exoskeleton used in the experiment simply relies on the EMG sensor without any physical sensors. This situation is not good for the user's safety because the EMG signal is dynamic and easy to change due to small movements. Therefore, physical sensors should be incorporated to anticipate the inability of the system to handle the changes of the EMG signals. Lastly, the experiments in this paper were conducted in able-bodied subjects. In future, the proposed MCS should be tested in the patients with various levels of severity of disability.

5. CONCLUSION

This paper proposed a novel MCS consisting of a new myoelectric pattern recognition using rejection-based extreme learning machine to predict the intended movements. The proposed new myoelectric pattern recognition (M-PR) employed radial basis function extreme learning machine with a rejection mechanism named RBF-ELM-R. The existence of the motion rejection mechanism improved the performance of the recognition system in both offline and online experiments. In the offline experiment, the MP-R achieved the accuracy of around 90% and 92% using RBF-ELM and RBF-ELM-R, respectively. The one-way ANOVA test results ($p = 0.034 < 0.05$) indicate that the improvement of RBF-ELM-R over RBF-ELM is significant. By selecting the proper rejection threshold, the accuracy of the M-PR using RBF-ELM-R can be improved.

In real-time application, the experiments involved the M-PR using RBF-ELM and RBF-ELM-R. The accuracy of the M-PR was about 89.22% and 89.73% for RBF-ELM and RBF-ELM-R, respectively. The efficacy of RBF-ELM-R was more noticeable if the classes that were not included in the training stage were involved in the test stage. When using 5 classes in the training stage and then in the testing phase, the other 5 classes were included, the MCS attained the accuracy of about 59% and 80% for RBF-ELM and RBF-ELM-R, respectively.

REFERENCES

[1] X. S. Li, *et al.*, "Analysis and simplification of three-dimensional space vector PWM for three-phase four-leg inverters," *IEEE Transactions on Industrial Electronics,* vol. 58, pp. 450-464, February 2011.

[2] Australian Bureau of Statistics, "4429.0 - Profiles of Disability, Australia, 2009," 2012. [Online]. Available: https://www.abs.gov.au/ausstats/abs@.nsf/Lookup/4429.0main+features100142009

[3] K. H. Low, "Robot-assisted gait rehabilitation: From exoskeletons to gait systems," *Defense Sci. Research Conf. and Expo (DSR)*, pp. 1-10, August 2011.

[4] R. Lu, Z. Li, C.-Y. Su, and A. Xue, "Development and learning control of a human limb with a rehabilitation exoskeleton," *IEEE Transactions on Industrial Electronics*, vol. 61, no. 7, pp. 3776-3785, July 2014.

[5] Z. Li, C. Y. Su, L. Wang, Z. Chen, and T. Chai, "Nonlinear disturbance observer-based control design for a robotic exoskeleton incorporating fuzzy approximation," *IEEE Transactions on Industrial Electronics*, vol. 62, no. 9, pp. 5763-5775, September 2015.

[6] Marc G. C., Dikai Liu, "Towards using Musculoskeletal Models for Intelligent Control of Physically Assistive Robots," *2011 Annual International of the IEEE Engineering in Medicine and Biology Society,* September 2011.

[7] L. L. Cai, *et al.*, "Implications of assist-as-needed robotic step training after a complete spinal cord injury on intrinsic strategies of motor learning," *Journal of Neuroscience*, vol. 26, no. 41, pp. 10564-10568, November 2006.

[8] M. Asghari Oskoei and H. Hu, "Myoelectric control systems-A survey," *Biomedical Signal Processing and Control*, vol. 2, no. 4, pp. 275-294, October 2007.

[9] E. E. Cavallaro, J. Rosen, J. C. Perry, and S. Burns, "Real-time myoprocessors for a neural controlled powered exoskeleton arm," *IEEE Transactions on Biomedical Engineering*, vol. 53, no. 11, pp. 2387-2396, November 2006.

[10] K. Kiguchi and Y. Hayashi, "An EMG-based control for an upper-limb power-assist exoskeleton robot," *IEEE Transactions on Systems, Man, and Cybernetics,* vol. 42, no. 4, August 2012.

[11] T. Triwiyanto, *et al.*, "Embedded system for upper-limb exoskeleton based on electromyography control," *TELKOMNIKA Telecommunication Computing Electronics and Control*, vol. 17, no. 6, pp. 2992-3002, 2019.

[12] S. A. Dalley, H. A. Varol, and M. Goldfarb, "A method for the control of multigrasp myoelectric prosthetic hands," *IEEE Transactions on Neural Systems and Rehabilitation Engineering*, vol. 20, no.1, pp. 58-67, December 2012.

[13] S. W. Lee, *et al.*, "Subject-specific myoelectric pattern classification of functional hand movements for stroke survivors," vol. 19, no. 5, pp. 558-566, October 2011.

[14] M. S. Park, K. Kim, and S. R. Oh, "A fast classification system for decoding of human hand configurations using multi-channel sEMG signals," *IEEE International Workshop on Intelligent Robots and Systems (IROS)*, pp. 4483-4487, September 2011.

[15] G. Matrone, C. Cipriani, M. C. Carrozza, and G. Magenes, "Two-channel real-time EMG control of a dexterous hand prosthesis," *Proc. 5th Int. IEEE/EMBS Conf. Neural Engineering (NER)*, pp. 554-557, May 2011.

[16] C. Cipriani, *et al.*, "Online myoelectric control of a dexterous hand prosthesis by transradial amputees," *IEEE Transactions on Neural Systems and Rehabilitation Engineering*, vol. 19, no.3, pp. 260-270, June 2011.

[17] S. Micera, J. Carpaneto, and S. Raspopovic, "Control of hand prostheses using peripheral information," *IEEE Reviews in Biomedical Engineering*, vol. 3, pp. 48-68, January 2010.

[18] J. Too, *et al.*, "Application of gabor transform in the classification of myoelectric signal," *TELKOMNIKA Telecommunication Computing Electronics and Control*, vol. 17, no. 2, pp. 873-881, April 2019.

[19] E. F. Shair, *et al.*, "Determining best window size for an improved gabor transform in EMG signal analysis," *TELKOMNIKA Telecommunication Computing Electronics and Control*, vol. 16, no. 4, pp. 1650-1658, August 2018.

[20] H. Huang, F. Zhang, Y. L. Sun, and H. He, "Design of a robust EMG sensing interface for pattern classification," *Journal of neural engineering*, vol. 7, no. 5, October 2010.
[21] H. Huang, T. A. Kuiken, and R. D. Lipschutz, "A strategy for identifying locomotion modes using surface electromyography," *IEEE Transactions on Biomedical Engineering*, vol. 56, no. 1, pp. 65-73, January 2009.
[22] M. Mulas, M. Folgheraiter, and G. Gini, "An EMG-controlled exoskeleton for hand rehabilitation," *Proceedings of the 2005 IEEE 9th International Conference on Rehabilitation Robotics*, July 2005.
[23] A. Wege and A. Zimmermann, "Electromyography sensor based control for a hand exoskeleton," *2007 IEEE International Conference on Robotics and Biomimetics, ROBIO*, December 2007.
[24] N. S. K. Ho, *et al.*, "An EMG-driven exoskeleton hand robotic training device on chronic stroke subjects: Task training system for stroke rehabilitation," *IEEE International Conference on Rehabilitation Robotics*, July 2011.
[25] E. J. Scheme, B. S. Hudgins, and K. B. Englehart, "Confidence-based rejection for improved pattern recognition myoelectric control," *IEEE Transactions on Biomedical Engineering*, vol. 60, no. 6, pp. 1563-1570, June 2013.
[26] G. Bin Huang, *et al*., "Extreme learning machine for regression and multiclass classification," *IEEE Transactions on Systems, Man, and Cybernetics, Part B: Cybernetics*, vol. 42, no. 2, April 2012.
[27] K. Anam and A. Al-Jumaily, "Swarm-based extreme learning machine for finger movement recognition," *Middle East Conference on Biomedical Engineering, MECBME*, pp. 273–276, February 2014.
[28] K. Anam, R. N. R. Khushaba, and A. Al-Jumaily, "Two-channel surface electromyography for individual and combined finger movements," pp. 4961-4964, July 2013.
[29] O. Fukuda, T. Tsuji, M. Kaneko, and A. Otsuka, "A human-assisting manipulator teleoperated by EMG signals and arm motions," *IEEE Trans. Robot. Autom.*, vol. 19, no. 2, pp. 210-222, April 2003.
[30] D. Tkach, H. Huang, and T. A. Kuiken, "Study of stability of time-domain features for electromyographic pattern recognition," *Journal of NeuroEngineering and Rehabilitation*, vol. 7, no. 1, May 2010.
[31] R. N. Khushaba, *et al.*, "Toward improved control of prosthetic fingers using surface electromyogram (EMG) signals," *Expert Systems with Applications*, vol. 39, no. 12, pp. 10731-10738, September 2012.
[32] D. Cai, X. He, and J. Han, "SRDA: An efficient algorithm for large scale discriminant analysis," *IEEE Transactions on Knowledge and Data Engineering*, vol. 20,no. 1, pp.1-12, January 2008.
[33] K. Englehart, B. Hudgins, and A. D. C. Chan, "Continuous multifunction myoelectric control using pattern recognition," *Technology and Disability*, vol. 15, no. 2, pp. 95-103, January 2003.
[34] M. A. Rahman and A. Al-Jumaily, "Design and development of a hand exoskeleton for rehabilitation following stroke," *Procedia Engineering*, vol. 41, pp. 1028-1034, 2012.

BIOGRAPHIES OF AUTHORS

Khairul Anam was born in Buleleng-Bali on the 5th of April 1978. He received his B.Eng. degree from the Department of Electrical Engineering, University of Brawijaya, in 2002; M.Eng. degree from the Institut Teknologi Sepuluh Nopember (ITS) Surabaya in 2008; and Ph.D. degree from the University of Technology, Sydney, Australia, in 2016. He is currently a Senior Lecturer in the Department of Electrical Engineering, University of Jember, Indonesia. His main interest is artificial intelligence and its application in electrical engineering, biomedical engineering, and other fields.

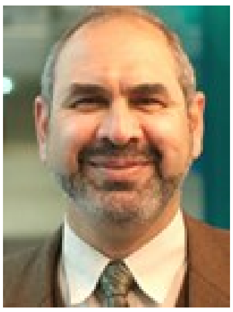

Dr. Adel Al-Jumaily received his B.SC. (Eng.) in Electrical Engineering and Education and M.SC. in Engineering Management from UT Bagdad and Ph.D. in Electrical Engineering from UTM Malaysia. Currently, he is an Associate Professor in the University of Technology Sydney. His research interest is in the fields of computational intelligence, bio-mechatronics systems, health technology and biomedical, vision-based cancer diagnosing, and artificial intelligent systems.